Chemical Science

ROYAL SOCIETY OF CHEMISTRY

EDGE ARTICLE

View Article Online
View Journal



Cite this: DOI: 10.1039/d4sc02214a

All publication charges for this article have been paid for by the Royal Society of Chemistry

# A Pd-catalyzed route to carborane-fused boron heterocycles†

Mengjie Zhu,[a] Puzhao Wang,[a] Zhengqiu Wu,[b] Yangfa Zhong,[a] Laiman Su,[e] Yuquan Xin,[a] Alexander M. Spokoyny, *[cd] Chao Zou *[b] and Xin Mu *[a]

Received 3rd April 2024
Accepted 28th May 2024

DOI: 10.1039/d4sc02214a

rsc.li/chemical-science

Due to the expanding applications of icosahedral carboranes in medicinal and materials chemistry research, their functionalizations have become one of the central themes in boron-rich cluster chemistry. Although several strategies for incorporating nitrogen-containing nucleophiles on a single boron vertex of the icosahedral carboranes ($C_2B_{10}H_{12}$) have been developed, methods for preparing clusters with vicinal B–N moieties are still lacking. The steric bulk of icosahedral carboranes and disparate electronic and steric nature of the N-containing groups have rendered the vicinal diamination challenging. In this article, we show how a developed Pd-catalyzed process is used to incorporate an array of NH-heterocycles, anilines, and heteroanilines with various electronic and steric profiles onto the vicinal boron vertices of a *meta*-carborane cluster *via* sequential or one-pot fashion. Importantly, oxidative cyclizations of the cross-coupling products with indoles and pyrroles appended to boron vertices generate a previously unknown class of all-boron-vertex bound carborane-fused six- and seven-membered ring heterocycles. Photophysical studies of the *meta*-carborane-fused heterocycles show that these structures can exhibit luminescence with high quantum yields and are amenable to further manipulations.

## Introduction

Difunctionalization of two-dimensional aromatic compounds to generate vicinal C–N bonds has proved to be a powerful strategy to increase molecular complexity,[1] and these *ortho*-diamine moieties have been found in natural products, pharmaceuticals, and multifunctional polymers.[2] In these structures, arene or heteroarene rings are crucial for supporting the N-substituents, and the proximity of these polar groups is usually essential to confer high-affinity binding interactions with biological targets (Fig. 1A, left).[3] Generally considered as three-dimensional analogs of benzene,[4] but with significantly larger van der Waals volume (143 Å for *meta*-carborane and 79 Å for benzene),[5] icosahedral *closo*-dicarbaboranes (colloquially referred to as carboranes) represent an important subset of boron-rich clusters and are emerging as interesting pharmacophore alternatives for drug discovery,[5b,6] and especially boron neutron capture therapy (BNCT) agents that require a significant payload of boron.[7] Functionalized carborane-based compounds can also present opportunities for the construction of new classes of functional materials and catalysts in which the inherent three-dimensionality of the building block is structurally and/or functionally necessary.[8] Thus, site-selective boron vertex-difunctionalization of icosahedral carboranes to install vicinal NH-heterocycles and other N-containing nucleophiles is highly desired in new research frontiers (Fig. 1A, right).

Early development of icosahedral carborane chemistry relied heavily on deprotonation reactions of relatively acidic C–H vertices ($pK_a \sim 20$ for icosahedral *ortho*-carborane) followed by the nucleophilic substitutions of the corresponding *C*-carboranyl species.[9] Recently, two complementary strategies have emerged as the mainstay of icosahedral carborane functionalizations on boron-based vertices: transition metal-catalyzed carborane B–H bond activation[10] and metal-catalyzed or mediated cross-coupling reactions between halogenated carboranes and nucleophiles.[11] For the cross-coupling route, although the reaction pattern is reminiscent of transition metal-catalyzed cross-couplings between organic electrophiles and nucleophiles, the intrinsic low reactivity driven by steric bulk of the surface B–halogen bonds on carboranes has made these transformations uniquely challenging and distinct from their

[a]Engineering Research Center of Pharmaceutical Process Chemistry, Ministry of Education, School of Pharmacy, East China University of Science and Technology, 130 Meilong Road, 200237, Shanghai, China. E-mail: xinmu@ecust.edu.cn

[b]Functional Coordination Material Group-Frontier Research Center, Songshan Lake Materials Laboratory, Dongguan, Dongguan 523808, Guangdong, China. E-mail: zouchao@sslab.org.cn

[c]Department of Chemistry and Biochemistry, University of California, Los Angeles, 607 Charles E. Young Drive East, Los Angeles, California 90095, USA

[d]California NanoSystems Institute (CNSI), University of California, Los Angeles, Los Angeles, California 90095, USA. E-mail: spokoyny@chem.ucla.edu

[e]School of Biotechnology, East China University of Science and Technology, 130 Meilong Road, 200237, Shanghai, China

† Electronic supplementary information (ESI) available. CCDC 2323379, 2323380, 2323386–2323391, 2323393, 2323397 and 2323399. For ESI and crystallographic data in CIF or other electronic format see DOI: https://doi.org/10.1039/d4sc02214a

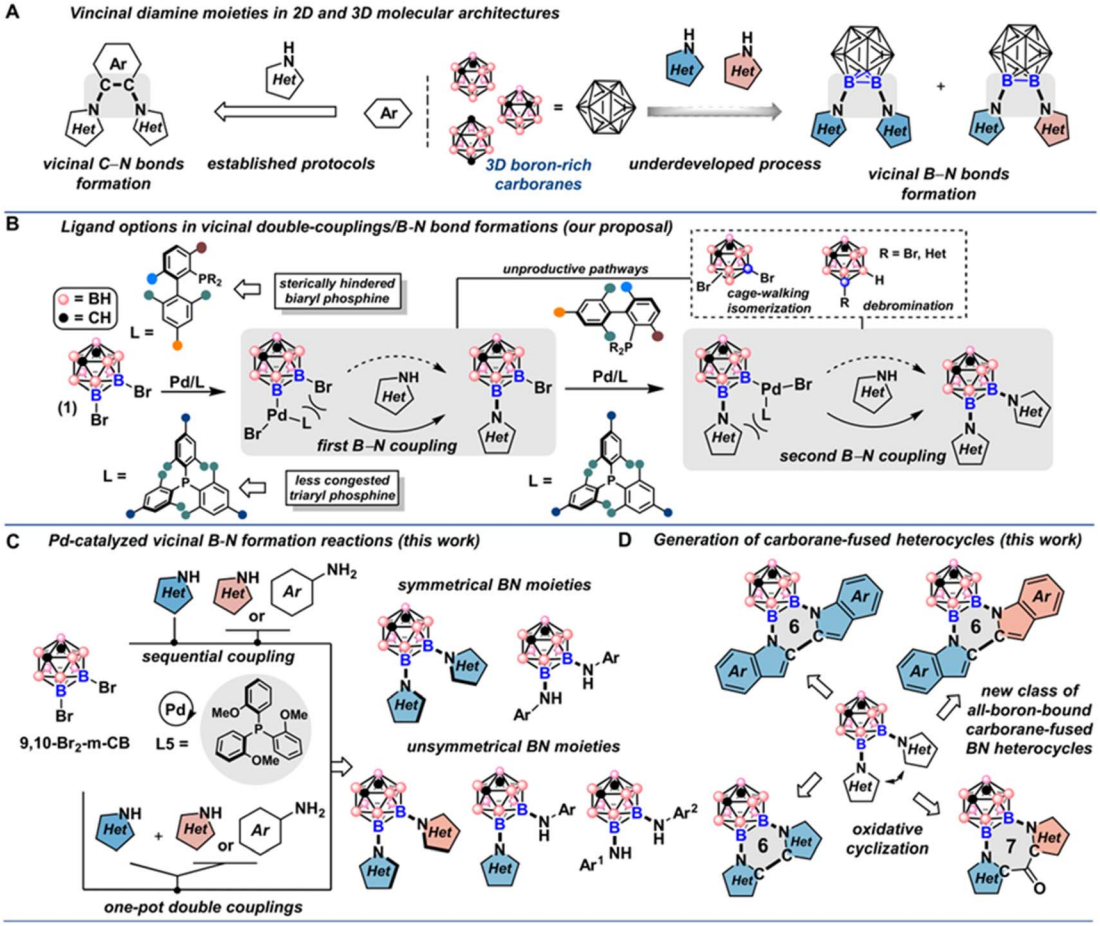


Fig. 1 (A) Established preparations for *o*-phenylene diamine structures and synthetically challenging carborane vicinal diamine structures for generating N–B–B–N moieties. (B) In Pd-catalyzed diamination reactions using 9,10-$Br_2$-*m*-carborane **1** and heterocycles, the sterically hindered biaryl monophosphine ligand could be detrimental to both coupling steps; triaryl phosphines serve as alternative less bulky ligands and lead to the desired products. (C) Our developed reaction sequence of preparing symmetrical and unsymmetrical diaminated products using the sequential or one-pot cross-coupling protocol using **L5** as the optimal ligand. (D) The oxidative cyclization of the double cross-coupling products affords previously unknown all-boron-vertex-bound carborane-fused six- and seven-membered rings.

arene-based counterparts. Furthermore, considering that icosahedral *ortho*- and *meta*-carborane isomers have a distinct propensity to undergo nucleophilic deboronation, the resulting nido-carborane species have been shown to poison catalytic Pd-based species, presenting an additional challenge in this chemistry.[12] Historically, boron-functionalized iodo-carboranes were first used as the coupling partners in Pd-catalyzed cross-coupling reactions due to the relatively weak B–I bond strength compared to the corresponding B–Br/Cl bonds, where Hawthorne and coworkers reported early examples of Pd-catalyzed amination of *meta* and *ortho* iodo-carboranes under mild conditions.[13] In 2016, icosahedral B-bromocarboranes were discovered to undergo efficient Pd-catalyzed cross-coupling reactions by employing bulky electron-rich biaryl monophosphine ligands to support catalytically active species.[12,14,15] Despite the demonstration that this catalytic reaction can engage B-bromocarboranes with several N-based and other nucleophiles, methods for incorporating vicinal B–N bond on carborane boron vertices are still challenging due to the steric bulk of the carborane scaffold and the steric hindrance from the incoming NH-heterocycles; and for the transition metal-catalyzed B–H bond activation strategy specifically, only one B–N bond can be produced using electrophilic aminating reagents and several electron-poor sulfonyl azides as the nitrogen source, leaving a large swath of electron-rich NH-heterocycles unavailable for the carborane B–N bond formation.[16,11e]

To achieve vicinal diamination of icosahedral carboranes, we employed 9,10-$Br_2$-*meta*-carborane **1** as the model electrophile and explored the feasibility of double cross-coupling reactions with NH-heterocycles. In addition to the points described above, several underlying challenges in the context of the proposed cross-coupling chemistry need to be considered: (1) although beneficial in the amination of 9-Br-*meta*-carboranes, use of electron-rich biaryl mono-phosphine ligands could be deleterious in this double cross-coupling reaction due to the significant steric clash with the neighboring B–Br bond in the first B–N couplings as well as the B–N couplings in the second step; (2) potential B–Br bond isomerization (*via* cage-walking) and debromination pathways induced by the use of biaryl

mono-phosphine ligands further complicate the reaction outcome (Fig. 1B, top).[12,15] Nonetheless, many NH-heterocycles are considered weakly coordinating nucleophiles towards the Pd(II) center after the oxidative addition step, and bulky phosphine ligands are often required for successful reductive elimination.[1c] We surmised that the electron-rich tri-arylphosphine ligands could serve as competent ligand scaffolds to achieve the vicinal B–N bond formations (Fig. 1B, bottom). In this report, we have successfully identified a solution to the Pd-catalyzed double cross-couplings of 9,10-$Br_2$-*meta*-carborane with diverse NH-heterocycles, anilines, and hetero-anilines. We showed that by utilizing a trisubstituted triarylphosphine ligand to support Pd-based catalysts, one can incorporate structurally diverse indoles, carbazoles, pyrroles and anilines onto the carborane neighboring B(9) and B(10) positions. Substrates containing additional coordinating sites such as pyrazoles and aminopyridines are compatible under the developed conditions. Importantly, symmetrical double cross-coupling products can be obtained with excess nucleophiles (Fig. 1C, top). Unsymmetrical doubly cross-coupled products can also be produced sequentially by isolating the mono-substituted intermediate and subjecting it to a second round of cross-coupling with a different nucleophile. Notably, two NH-heterocycles and anilines of disparate electronic and steric profiles can be installed in a one-pot fashion (Fig. 1C, bottom). Additionally, we were able to develop efficient protocols for oxidative couplings of the C-2 positions of vicinal indoles and pyrroles appended to B-based vertices in icosahedral *meta*-carboranes (Fig. 1D). This yielded previously unknown all-boron-vertex-bound carborane-fused six- and seven-membered ring heterocycles. Photophysical studies of carborane-fused heterocycles show that these new heterocyclic structures can exhibit high photoluminescence quantum yields.

## Results and discussion

### Ligand screening

By employing 9,10-$Br_2$-*meta*-carborane **1** and indole **N1** as the cross-coupling partners, we examined a series of mono- and di-phosphine ligands (Fig. 2, for details of the reaction screening, see Table S1†). Besides the desired product **2a**, mono-substituted product **2b** and debromination byproduct **3** were also obtained during the ligand screening. Biaryl mono-phosphine ligands **L1–L3** all gave **2a** in low yields. 2-Dicyclohexylphosphino-2′,4′,6′-triisopropylbiphenyl (Xphos, **L1**) generated slightly more **2b** than when **L2** and **L3** were employed. Utilizing **L4** bearing a carbazole group also produced **2b** as the main product. Triarylphosphine ligands **L5–L7** bearing different numbers of electron-rich groups led to divergent product distributions. For **L5** with three *ortho*-methoxyl groups, **2a** was obtained in 73% GC yield (75% isolated yield) with minimal by-product generation. In contrast, **L7** with three *ortho*-methyl groups instead of OMe produced **2b** in only 34% yield as the major product. To our surprise, diminished reactivity was observed when **L6** with two additional MeO groups compared to **L5** was tested. This result indicates that both electronic and steric factors intricately contribute to the

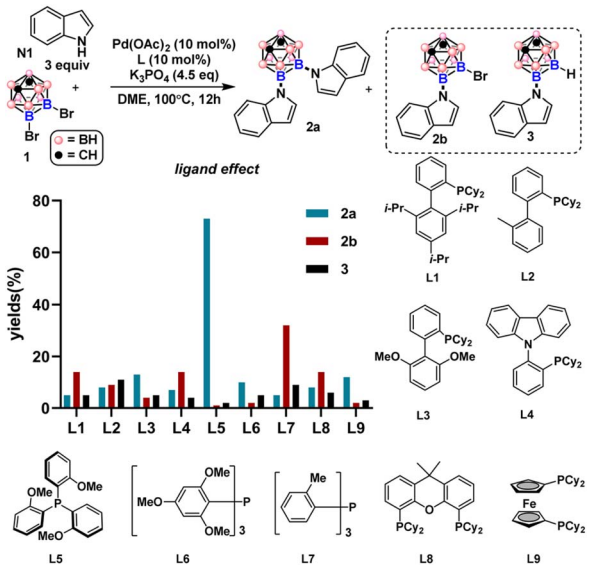


Fig. 2 Ligand screening for the Pd-catalyzed double cross-coupling reactions between **1** and indole **N1**. Reaction conditions: 9,10-$Br_2$-*meta*-carborane **1** (0.1 mmol, 1.0 equiv.), indole (0.3 mmol, 3 equiv.), 10 mol% $Pd(OAc)_2$ (0.01 mmol, 10 mol%), 20 mol% ligands (0.02 mmol, 20 mol%) and 1 mL DME at 100 °C for 12 h under a $N_2$ atmosphere. The yields were determined by GC-MS analysis using decane as an internal standard.

efficiency of triarylphosphine ligands in the double cross-coupling reactions. Diphosphine ligand **L8** gave **2a** in low yields. For **L9**, higher selectivity for **2a** than **L8** was obtained, albeit with low reactivity.

### Substrate scope

Upon identifying **L5** as a suitable ligand choice, we first evaluated the generality of the developed catalytic system in the symmetrical double cross-couplings (Fig. 3). Indole and carbazole derivatives bearing electron-rich and electron-deficient functional groups are suitable nucleophiles in this reaction, furnishing the desired vicinal B–N moieties with good to excellent yields. Substrates with methoxy and benzyloxy groups at indole C-5 positions (**3a** and **4a**) gave 66% and 88% yields, respectively. Indole-5-carboxaldehyde is compatible under the developed conditions to give **6a** in 32% yield. Trifluoromethylated and fluorinated indoles are converted to the double cross-coupled products **7a** and **8a** in moderate yields. Indoles with C-4 substitution are also suitable coupling partners (**10a–13a**). It is worth noting that boronic acid pinacol esters can withstand the cross-coupling conditions. The structures of the double cross-coupling products were verified by $^1H$, $^{11}B/^{11}B\{^1H\}$, and $^{13}C\{^1H\}$ spectroscopy and high-resolution mass spectrometry (HRMS). The structural identity was also independently confirmed by single crystal X-ray diffraction experiments. Indoles bearing C-4 and C-5 nitrile groups are successfully converted to the corresponding products **14a** and **15a** in moderate to good yields. Carbazole and its derivatives were suitable substrates, and difunctionalized products **18a–21a** can be building blocks for potential applications in optical

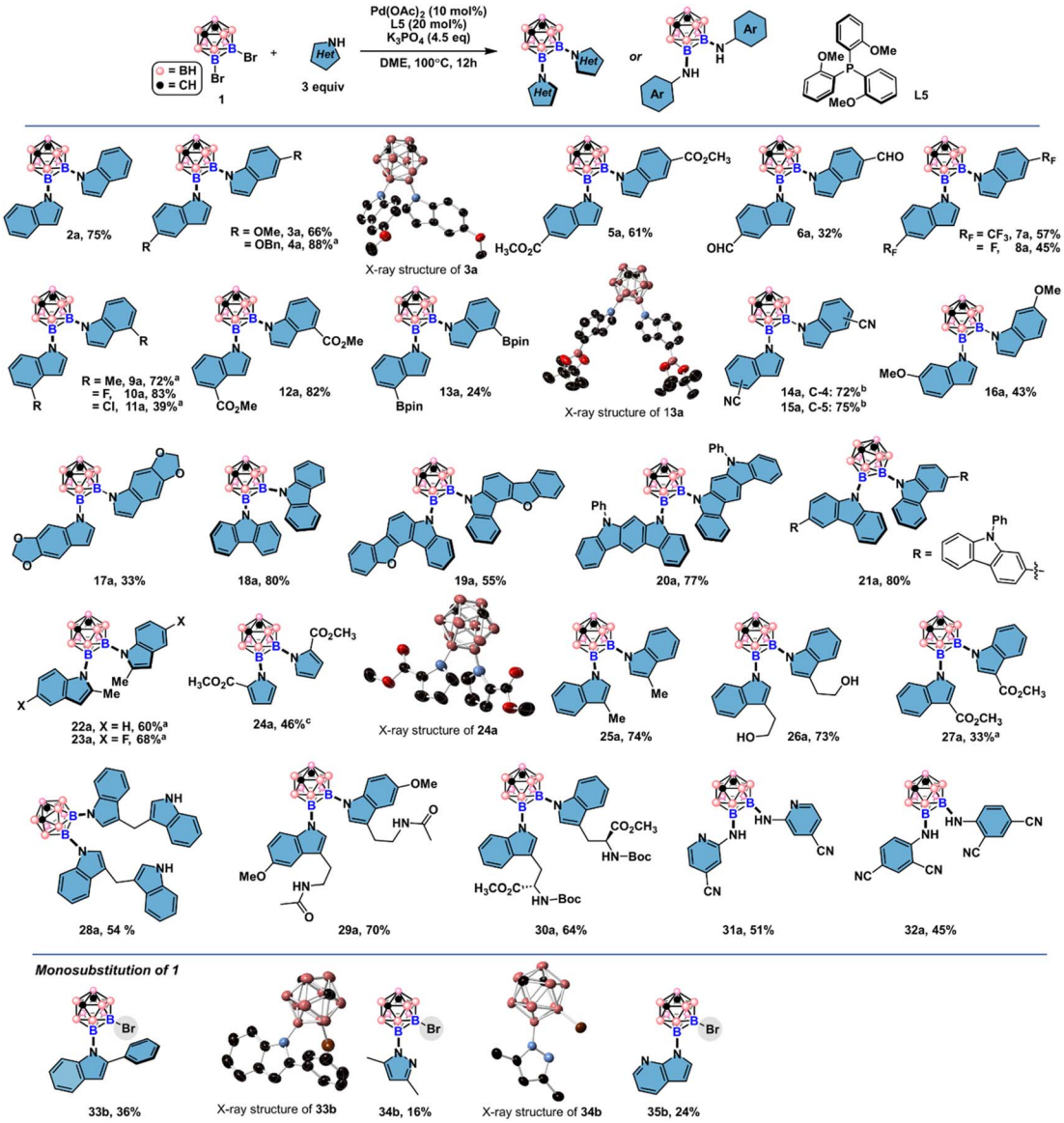


Fig. 3 Substrate scope of Pd-catalyzed symmetrical double cross-coupling reactions. Electron-rich and -poor indoles are compatible under the developed conditions. Reaction conditions: **1** (0.2 mmol, 1 equiv.), heterocycle (0.6 mmol, 3 equiv.), $Pd(OAc)_2$ (0.02 mmol, 10 mol%), **L5** (0.04 mmol, 20 mol%), $K_3PO_4$ (0.9 mmol, 4.5 equiv.), DME (0.1 M, 2.0 mL), $N_2$, 100 °C, 12 h. Ellipsoids at 50% probability and all H atoms in single crystal X-ray structures depicted are omitted for clarity. (a) Using *t*-BuONa as the base and dioxane as the solvent. (b) Using dioxane as the solvent. (c) Using 1,3-bis(dicyclohexylphosphino)propane as the ligand. See the ESI† for reaction details.

devices. The compatibility of this catalytic system with an array of indoles with diverse electronic features encouraged us to explore the functional group tolerance under the current conditions further. Sterically hindered indoles, challenging substrates in Pd-catalyzed C–N bond coupling reactions, were tested in the double cross-couplings with bulky B–Br bonds in **1**. Under the standard conditions, 2-methyl indoles gave **22a** and **23a** in 60% and 68% yields, respectively. These results represent rare examples of cross-couplings of carborane-containing electrophiles with sterically hindered nucleophiles. Methyl pyrrole 2-carboxylate was another suitable NH-heterocycle besides indoles and carbazoles for the double cross-couplings to give **24a** in 46% yield. Next, indoles with C-3 substitutions were examined. Reaction with ethyl indole-3-carboxylate gave **27a** in 33% yields, suggesting that the weak nucleophiles are unfavorable in the double cross-couplings since NH moieties are more susceptible to electronic variations on the pyrrole ring of indole substrates. Selective B–N over B–O bond formation was obtained when tryptophol with a free hydroxyl group was applied under the standard conditions, and the desired product **26a** was obtained in 73% yield. Under standard conditions, two 3,3′-diindolymethane (DIM) molecules were incorporated to produce **28a**, and unprotected NH moieties are compatible under the developed reaction conditions. There are two types of NH units in melatonin and tryptophan methyl ester, and only NH from the pyrrole ring reacted with 9,10-$Br_2$-*meta*-carborane

to give **29a** and **30a** in 70% and 64% yields, respectively. Additionally, two electron-deficient anilines were also reactive to give disubstituted carborane products **31a** and **32a** in moderate yields. Excellent functional group compatibility during the substrate screening prompted us to investigate the limitations of this protocol further. By using 2-phenyl indole, only a monosubstitution product **33b** was obtained in 36% yield. 2,4-Dimethyl pyrazole and 7-azaindole are challenging coupling partners for the symmetrical double cross-couplings. Complex reaction mixtures were observed, and we only isolated monosubstituted products **34b** and **35b** in low yields. The structural assignments of **34b** and **35b** were confirmed by single crystal X-ray crystallography. These results might be attributed to the extra basic nitrogen coordination sites for the Pd catalyst from pyrazole and 7-azaindole that impeded the second-round cross-coupling reactions.

Unsymmetrical difunctionalization would be an ideal strategy for rapidly increasing icosahedral carborane diversity as building blocks in materials and three-dimensional pharmacophores.[6m,7b,7i,8k] However, existing methods are not capable of introducing two NH-heterocycles and anilines of different electronic and steric characteristics.[16] First, we prepared the monosubstituted product **3b** in 62% yield using 5-methoxyindole and 1.2 equivalents of 9,10-$Br_2$-*meta*-carborane **1**. Next, we tested an array of NH-heterocycles, including 3,5-dimethyl-pyrazole, methyl 2-pyrrolecarboxylate, substituted indoles, 7-azaindole, and aniline derivatives for the second-round cross-couplings. All tested coupling partners were successfully converted to the desired products in moderate to good yields (Fig. 4).

The structures of **37a** and **42a** were also crystallographically determined which are consistent with the structural assignment from the proton and heteronuclear NMR spectroscopy. It is noteworthy that 3,5-dimethyl-pyrazole and 7-azaindole, unsuitable for symmetrical double couplings, were successfully incorporated by reacting with **3b** under slightly tuned reaction conditions. With 2,4-dicyanoaniline as the second nucleophile, diaminated *meta*-carborane **43a** was obtained in 61% yield. These encouraging results prompted us to explore whether unsymmetrical double cross-couplings could be achieved in a one-pot fashion (Fig. 5). The combination of electron-rich indoles, carbazole derivatives with electron-deficient indoles or anilines gave the unsymmetrically disubstituted carboranes in one step (**44a–52a**). Anilines of disparate electronic characteristics are also operational coupling combinations to produce the desired results (**51a–52a**). Exceptional functional group compatibility was displayed when tryptophol and *tert*-butyl carbamate was added in one pot as the nucleophiles. Both free hydroxyl from tryptophol and NH group from the carbamate were retained and can be subjected to further manipulations (**50a**).

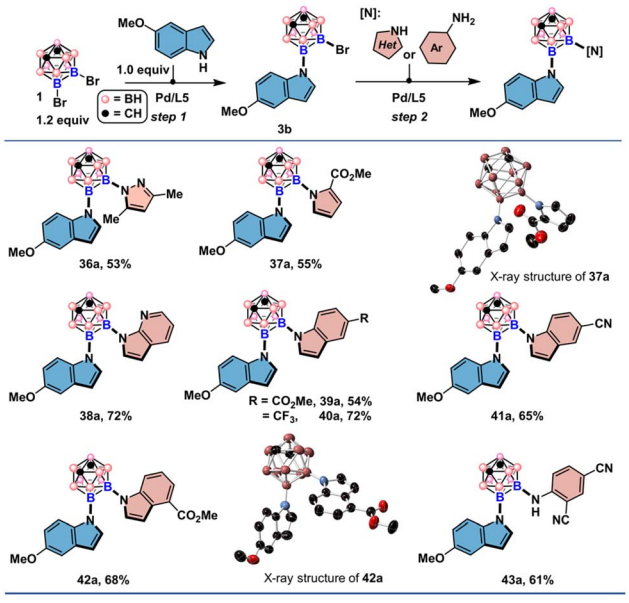


Fig. 4 Substrate scope of sequential Pd-catalyzed un-symmetrical double cross-coupling reactions. See the ESI† for the reaction details. All H atoms in single crystal X-ray structures depicted are omitted for clarity.

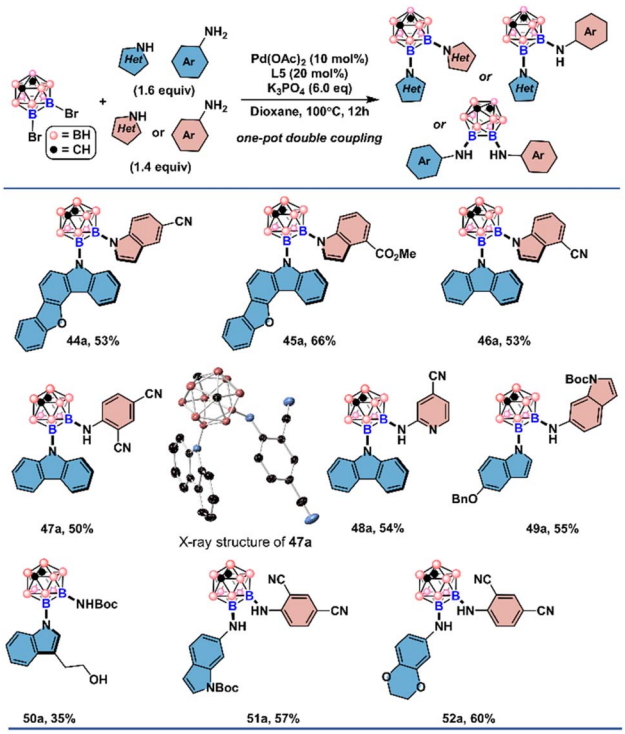


Fig. 5 Substrate scope of one-pot Pd-catalyzed un-symmetrical double cross-coupling reactions. See the ESI† for the reaction details. All H atoms in single crystal X-ray structures depicted are omitted for clarity.

## Synthesis of carborane-fused heterocycles

Several previous studies have been dedicated to generating icosahedral carborane-fused 2D carbo- and hetero-cycles as extensions of the carborane scaffolds.[17] These systems are interesting as they can provide new insights into questions of electronic delocalization between 2D and 3D aromatic scaffolds and give rise to structurally new heterocyclic motifs.[18] However,

all-boron-vertex-bound icosahedral carborane-fused heterocycles bearing vicinal B–N bonds are still not accessible so far. We proposed that the spatial proximity of the indole and pyrrole C-2 positions after the double cross-couplings might be beneficial for the oxidative coupling reaction to synthesize a new class of all-boron-vertex-bound *meta*-carborane-fused heterocycles. By using $I_2$ as the oxidant and dichloroethane as the solvent, icosahedral *meta*-carborane-fused six-membered heterocycles **53–58** were prepared in good to excellent yields from symmetrically and unsymmetrically cross-coupled products using indole and its derivatives (Fig. 6A). The X-ray single crystal structure of **53** suggests a coplanar geometry of the newly formed six-membered ring and neighboring indole moieties (Fig. 6B). The B(9)–B(10) bond length of the resulting heterocycle is shorter than that of its uncyclized counterparts (1.754(6) Å, compared to 1.825(2) Å for **42a** and 1.8520(19) Å for **47a**). The slight contraction of the B–B bond length may be attributed to the ring strain of the planar hexagon configuration. Both N(1)–B(9)–B(10)/N(2)–B(10)–B(9) angles are smaller than 120° (113.8° and 114.5°, respectively), and the deviation is more significant than C(2)–C(1)–N(1)/C(1)–C(2)–N(2) angles, which are slightly larger than 120° (122.6° and 123.2°, respectively). The co-planar geometry of **53** with the sum of internal hexagonal angles being nearly 720° could be indicative of some degree of aromatic features. The downfield shift of carborane CH proton signal from 3.04 ppm for **2a** to 3.11 ppm for **53** suggests a small deshielding effect from the all-boron vertex bound six-membered heterocycle. It is noteworthy that **37a**, containing one indole and one substituted pyrrole unit was also successfully cyclized to give **59** in excellent yield under the developed cyclization conditions. Interestingly, when substrate **24a** with two C-2 methyl ester-substituted pyrroles was subjected to the same conditions, a formal Friedel–Crafts type acylation took place, and white solids with the carborane-fused seven-membered ring **60** were isolated and characterized by the NMR spectroscopy and single crystal X-ray crystallography. In the crystal structure, the B–B bond length of the heterocycle is 1.778(2) Å, longer than that of **53** (1.754(6) Å), indicating a reduced ring strain configuration. B(9)–N(1) is slightly longer than B(10)–N2 (1.5088(19) Å *versus*. 1.483(2) Å), which can be attributed to the steric and effects from the methyl ester group (Fig. 6C). The seven-membered ring bent towards the carborane moiety and the dihedral angle between the N(2)–B(10)–B(9)–N(1) and N(2)–N(1)–C(2) planes is 144°, strongly deviating from a coplanar geometry. When cerium(IV) ammonium nitrate (CAN) was used as the oxidant, a dark red solid was obtained. The structure of the dark red solid was identified as **61** with a carborane-fused six-membered ring and one nitro group on each pyrrole ring (Fig. 6D). In the crystal structure of **61**, a twisted hexagon was obtained with 15° twisting angle. The B(9)–B(10) bond is the longest among the three crystal structures (1.794(3) Å compared to 1.778(2) Å for **60** and 1.754(6) Å for **53**).

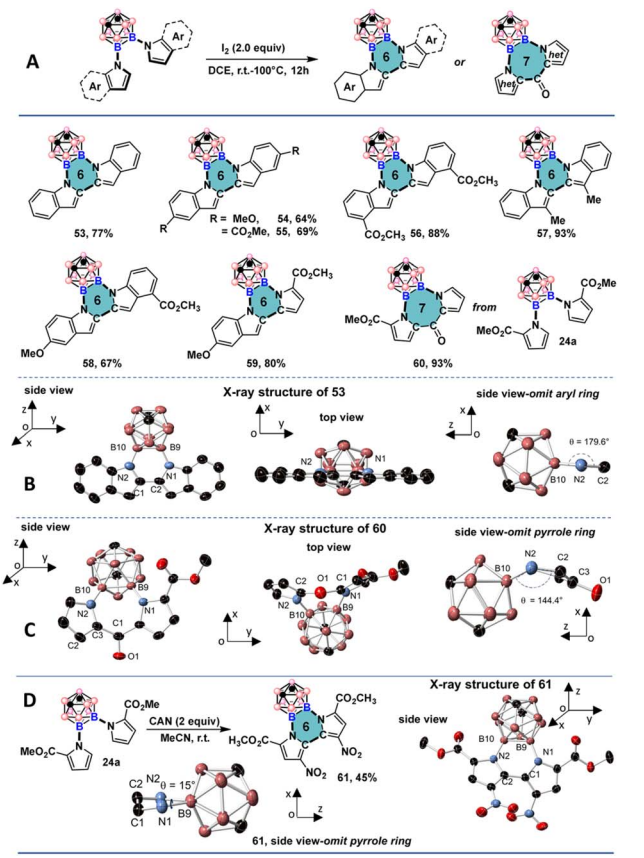


Fig. 6 The developed protocols for the synthesis of all-boron-vertex-bound *meta*-carborane-fused heterocycles. (A) In the presence of $I_2$, six- and seven-membered carborane-fused heterocycles are generated. (B) Different angles of view of the X-ray single crystal structure of **53**, top and side views are provided. (C) Different angles of view of the X-ray single crystal structure of **60**, top and side views are provided. (D) By using CAN, a dinitro-substituted six-membered heterocycle was obtained. All H atoms in single crystal X-ray structures depicted are omitted for clarity.

## Photophysical studies

Having obtained the double cross-coupling products and carborane-fused heterocycles, we were keen to benchmark their fundamental photophysical properties. Photophysical data were gathered for compounds **12a**, **42a**, **56**, and **58** as a representative series (Fig. 7 and S10†). As depicted in Fig. 7A, the absorption spectrum of the oxidative-cyclization product **56** in the dichloromethane solution exhibits a significant redshift compared to that of **12a**. In addition, two new distinct fine-level absorption peaks emerge at 396 nm and 418 nm, while the low-energy absorption edge extends into the visible light range. This suggests an increase in the conjugation system of **56** relative to **12a**, leading to the corresponding redshifted emission peaks (from 390 nm for **12a** to 438 and 460 nm for **56**). The prominent vibrational emission peaks of **56** at 438 and 460 nm indicate a reduced level of structural distortion in its excited state due to its significantly higher rigidity than that of **12a** after oxidation-cyclization. Consequently, the corresponding absolute quantum yield (QY) in a dilute DCM solution also increases from 0.50 for **12a** to 0.79 for **56**. The absorption and emission spectra of both **12a** and **56** exhibit significant overlap and

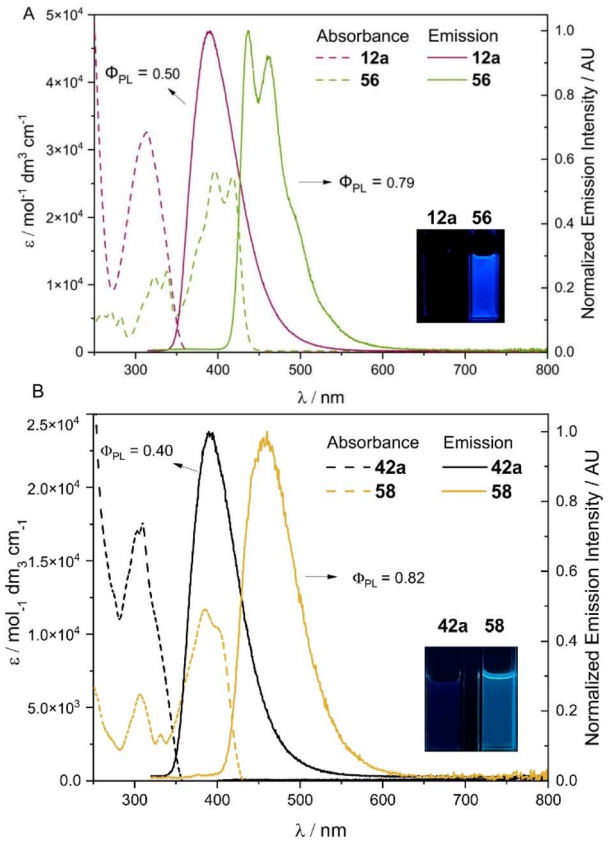


Fig. 7 Electronic absorption (dashed line) and emission spectra (solid line, excitation at 310 nm) in $CH_2Cl_2$ solution ($10^{-5}$ M) at room temperature in air, for compounds: (A) **12a** and its corresponding oxidative cyclization product **56**; (B) **42a** and corresponding oxidative cyclization product **58**. Photo insets are DCM solutions of **12a**, **56**, **42a** and **58** ($10^{-5}$ M, irradiated with UV light, $\lambda_{exc}$ = 365 nm).

a mirror relationship, respectively, and their emission lifetimes ($\tau$) are in the range of a few ns. Additionally, their short Stokes shifts suggest a fluorescent nature for these radiative decays. The emission peak (388 nm) and shape of the **12a** solid sample are generally consistent with its single-molecule fluorescence in dilute solution, while the emission peaks (470 and 500 nm) of the **56** solid shift noticeably to the red compared to its dilute solution (438 and 460 nm) (Fig. S16†). Moreover, the corresponding absolute QY of the **56** solid decreases more prominently than **12a** (0.24 for the **12a** solid and 0.05 for the **56** solid, see Table S15† for more details). This may be attributed to the well-arranged planar fused-ring structures in **56**, which may tend to stack and exhibit aggregation-caused quenching (ACQ) effects in the solid state. For another pair of compounds, **42a** and its cyclized derivative **58**, a similar redshifted fluorescence pattern is observed for the unsymmetrically disubstituted product **42a** and its cyclized form **58** (from 390 nm to 460 nm, see Fig. 7B). Compound **42a** with 5-methoxy indole and 4-methyl indole carboxylate exhibits an absolute QY of 0.40 ($\tau$ = 5.6 ns), while the carborane-fused product **58** with a more rigid configuration yields an absolute QY of 0.82 ($\tau$ = 3.0 ns) in a dilute DCM solution. Overall, these results demonstrate that the new heterocyclic ring structures generated through connecting multiple boron vertices in carboranes *via* B–N bonds can exhibit different photoluminescence properties by changing substituents with diverse electronic effects on the NH-heterocycles.

## Conclusions

We have identified an efficient catalytic system using a Pd-catalyst supported by the tris(*o*-methoxyphenyl)phosphine ligand as the optimal system to synthesize a wide array of densely functionalized icosahedral *meta*-carboranes with vicinal B–N moieties. In this transformation, a variety of NH-heterocycles such as electron-rich and deficient indoles, carbazole and its derivatives, pyrroles and pyrazoles are compatible under the developed conditions. Anilines and heteroanilines are also competent cross-coupling partners in this transformation. Unsymmetrical double cross-couplings were achieved in both sequential and one-pot fashion. Sterically hindered indoles are also tolerated under the current conditions to generate disubstituted products. The developed strategy provides unprecedented functional group and steric tolerance compared to existing icosahedral carborane functionalization chemistry and sets the groundwork for poly-functionalization chemistry of icosahedral carboranes *via* metal-catalyzed cross-coupling chemistry. More importantly, oxidative cyclization of the cross-coupling products has allowed for the generation of a new class of previously inaccessible all-boron-vertex bound six- and seven-membered icosahedral carborane-fused heterocycles using either transition metal-catalyzed B–H bond functionalization or cross-coupling strategies. X-ray crystallographic analysis of the heterocycles disclosed several different structural configurations presented in these heterocyclic rings including coplanar, twisted six-membered ring and non-planar seven-membered ring structures. Photophysical investigations of the icosahedral *meta*-carborane-fused heterocycles indicated that these systems can exhibit luminescence with high quantum yields and are potentially amenable for extensive tuning resulting from the identity of the heterocycle appended onto a boron cluster cage. This work shows how metal-catalyzed cross-coupling can be applied towards unconventional and challenging substrates leading to the formation of never-before-seen heterocyclic motifs with interesting photophysical properties.

## Data availability

The datasets associated with this article are available in the ESI.† CCDC 2323379 (**3a**), 2323380 (**13a**), 2323386 (**24a**), 2323387 (**33b**), 2323388 (**34b**), 2323389 (**37a**), 2323390 (**42a**), 2323391 (**47a**), 2323393 (**53**), 2323397 (**60**), 2323399 (**61**) contain the supplementary crystallographic data for this paper.†

## Author contributions

X. M. designed and supervised the project. M. Z. performed reaction condition optimizations. M. Z. and P. W. explored the

substrate scope. C. Z. directed photophysical analysis. Z. W. collected the photophysical data. Y. Z., L. S. and Y. X. helped in collecting some experimental data. M. Z., P. W. and Z. W. prepared the ESI.† X. M., A. S. and C. Z. wrote and edited the manuscript. All authors analyzed the data and commented on the manuscript during its preparation.

## Conflicts of interest

There are no conflicts to declare.

## Acknowledgements

Support for this study was provided by Natural Science Foundation of Shanghai (22ZR1416700) and start-up fund from Songshan Lake materials Laboratory (Y1D1061C11). We thank Prof. Guosheng Liu and Dr Haoyang Wang from Shanghai Institute of Organic Chemistry for fruitful discussions. We are thankful for the financial support from Engineering Research Center of Pharmaceutical Process Chemistry, Ministry of Education.

## Notes and references

1 For reviews on generation of aryl C–N bonds see: (*a*) F. Terrier, *Modern Nucleophilic Aromatic Substitution*, Wiley-VCH, Weinheim, Germany, 2013; (*b*) C. Sambiagio, S. P. Marsden, A. J. Blacker and P. C. McGowan, *Chem. Soc. Rev.*, 2014, **43**, 3525–3550; (*c*) P. Ruiz-Castillo and S. L. Buchwald, *Chem. Rev.*, 2016, **116**, 12564–12649; (*d*) R. Dorel, C. P. Grugel and A. M. Haydl, *Angew. Chem., Int. Ed.*, 2019, **58**, 17118–17129. For recent examples of 1,2-aryl diamine synthesis, see: ; (*e*) S. Gonell, M. Poyatos and E. Peris, *Angew. Chem., Int. Ed.*, 2013, **52**, 7009–7013; (*f*) L. Li, D. Qiu, J. Shi and Y. Li, *Org. Lett.*, 2016, **18**, 3726–3729; (*g*) M. Xiong, Z. Gao, X. Liang, P. Cai, H. Zhu and Y. Pan, *Chem. Commun.*, 2018, **54**, 9679–9682; (*h*) R. Sánchez-Bento, B. Roure, J. Llaveria, A. Ruffoni and D. Leonori, *Chem*, 2023, **9**, 3685–3695.

2 For recent examples of vicinal diaminated arenes in medicinal research, see: (*a*) D. J. O'Neill, A. Adedoyin, J. A. Bray, D. C. Deecher, A. Fensome, J. A. Goldberg, J. Harrison, L. Leventhal, C. Mann, L. Mark, L. Nogle, N. R. Sullivan, T. B. Spangler, E. A. Terefenko, E. J. Trybulski, A. J. Uveges, A. Vu, G. T. Whiteside and P. Zhang, *J. Med. Chem.*, 2011, **54**, 6824–6831; (*b*) M. W. Karaman, S. Herrgard, D. K. Treiber, P. Gallant, C. E. Atteridge, B. T. Campbell, K. W. Chan, P. Ciceri, M. I. Davis, P. T. Edeen, R. Faraoni, M. Floyd, J. P. Hunt, D. J. Lockhart, Z. V. Milanov, M. J. Morrison, G. Pallares, H. K. Patel, S. Pritchard, L. M. Wodicka and P. P. Zarrinkar, *Nat. Biotechnol.*, 2008, **26**, 127–132. For reviews and recent applications of *ortho*-phenylene diamines in functional polymers, see: ; (*c*) X.-G. Li, M.-R. Huang, W. Duan and Y.-L. Yang, *Chem. Rev.*, 2002, **102**, 2925–3030; (*d*) Q. L. Guan, Y. Sun, R. Huo, Y. Xin, F. Y. Bai, Y. H. Xing and L. X. Sun, *Inorg. Chem.*, 2021, **60**, 2829–2838; (*e*) H. Zhang, S. H. Lam, Y. Guo, J. Yang, Y. Lu, L. Shao, B. Yang, L. Xiao and J. Wang, *ACS Appl. Mater. Interfaces*, 2021, **13**, 51855–51866; (*f*) S.-W. Kim, W. K. Lee and J.-S. Lee, *ACS Omega*, 2023, **8**, 46267–46275.

3 D. C. Blakemore, L. Castro, I. Churcher, D. C. Rees, A. W. Thomas, D. M. Wilson and A. Wood, *Nat. Chem.*, 2018, **10**, 383–394.

4 (*a*) W. N. Lipscomb, *Boron Hydrides*, Benjamin, New York, 1963; (*b*) P. V. R. Schleyer and K. Najafian, *Inorg. Chem.*, 1998, **37**, 3454–3470; (*c*) Z. Chen and R. B. King, *Chem. Rev.*, 2005, **105**, 3613–3642; (*d*) R. B. King, *Chem. Rev.*, 2001, **101**, 1119–1152.

5 (*a*) Y. H. Zhao, M. H. Abraham and A. M. Zissimos, *J. Org. Chem.*, 2003, **68**, 7368–7373; (*b*) M. Scholz and E. Hey-Hawkins, *Chem. Rev.*, 2011, **111**, 7035–7062.

6 For recent reviews on carboranes in medicinal research, see: (*a*) F. Issa, M. Kassiou and L. M. Rendina, *Chem. Rev.*, 2011, **111**, 5701–5722; (*b*) G. Detlef, *Pure Appl. Chem.*, 2015, **87**, 173–179; (*c*) Z. J. Leśnikowski, *J. Med. Chem.*, 2016, **59**, 7738–7758; (*d*) A. Marfavi, P. Kavianpour and L. M. Rendina, *Nat. Rev. Chem.*, 2022, **6**, 486–504. For selected recent applications of carboranes and boron clusters in medicinal chemistry, see: ; (*e*) R. L. Julius, O. K. Farha, J. Chiang, L. J. Perry and M. F. Hawthorne, *Proc. Natl. Acad. Sci. U. S. A.*, 2007, **104**, 4808–4813; (*f*) M. L. Beer, J. Lemon and J. F. Valliant, *J. Med. Chem.*, 2010, **53**, 8012–8020; (*g*) T. Goto, K. Ohta, S. Fujii, S. Ohta and Y. Endo, *J. Med. Chem.*, 2010, **53**, 4917–4926; (*h*) S. Fujii, K. Ohta, T. Goto, A. Oda, H. Masuno, Y. Endo and H. Kagechika, *Med. Chem. Commun.*, 2012, **3**, 680–684; (*i*) S. Fujii, A. Kano, C. Songkram, H. Masuno, Y. Taoda, E. Kawachi, T. Hirano, A. Tanatani and H. Kagechika, *Biorg. Med. Chem.*, 2014, **22**, 1227–1235; (*j*) S. M. Wilkinson, H. Gunosewoyo, M. L. Barron, A. Boucher, M. McDonnell, P. Turner, D. E. Morrison, M. R. Bennett, I. S. McGregor, L. M. Rendina and M. Kassiou, *ACS Chem. Neurosci.*, 2014, **5**, 335–339; (*k*) J. Balintová, A. Simonova, M. Białek-Pietras, A. Olejniczak, Z. J. Lesnikowski and M. Hocek, *Bioorg. Med. Chem. Lett.*, 2017, **27**, 4786–4788; (*l*) Y. Asawa, K. Nishida, K. Kawai, K. Domae, H. S. Ban, A. Kitazaki, H. Asami, J.-Y. Kohno, S. Okada, H. Tokuma, D. Sakano, S. Kume, M. Tanaka and H. Nakamura, *Bioconjug. Chem.*, 2021, **32**, 2377–2385; (*m*) D. Kodr, C. P. Yenice, A. Simonova, D. P. Saftić, R. Pohl, V. Sýkorová, M. Ortiz, L. Havran, M. Fojta, Z. J. Lesnikowski, C. K. O Sullivan and M. Hocek, *J. Am. Chem. Soc.*, 2021, **143**, 7124–7134; (*n*) R. Varkhedkar, F. Yang, R. Dontha, J. Zhang, J. Liu, B. Spingler, S. Van der Veen and S. Duttwyler, *ACS Cent. Sci.*, 2022, **8**, 322–331; (*o*) B. B. Jei, L. Yang and L. Ackermann, *Chem.–Eur. J.*, 2022, **28**, e202200811; (*p*) A. R. Genady, J. Tan, M. E. El-Zaria, A. Zlitni, N. Janzen and J. F. Valliant, *J. Organomet. Chem.*, 2015, **791**, 204–213; (*q*) A. S. Louie, N. Vasdev and J. F. Valliant, *J. Med. Chem.*, 2011, **54**, 3360–3367.

7 For recent reviews on BNCT treatment using carboranes, see: (*a*) G. Calabrese, A. Daou, E. Barbu and J. Tsibouklis, *Drug Discov. Today*, 2018, **23**, 63–75; (*b*) D. J. Worm, P. Hoppenz, S. Els-Heindl, M. Kellert, R. Kuhnert, S. Saretz,

 

J. Köbberling, B. Riedl, E. Hey-Hawkins and A. G. Beck-Sickinger, *J. Med. Chem.*, 2020, **63**, 2358–2371; (*c*) M. A. Dymova, S. Y. Taskaev, V. A. Richter and E. V. Kuligina, *Cancer Commun.*, 2020, **40**, 406–421; (*d*) F. Ali, N. S. Hosmane and Y. Zhu, *Molecules*, 2020, **25**, 828; (*e*) T. D. Malouff, D. S. Seneviratne, D. K. Ebner, W. C. Stross, M. R. Waddle, D. M. Trifiletti and S. Krishnan, *Front. Oncol.*, 2021, **11**, DOI: 10.3389/fonc.2021.601820, Review.; (*f*) Y. Chen, F. Du, L. Tang, J. Xu, Y. Zhao, X. Wu, M. Li, J. Shen, Q. Wen, C. H. Cho and Z. Xiao, *Mol. Ther. Oncolytics.*, 2022, **24**, 400–416; (*g*) T. D. Marforio, A. Carboni and M. Calvaresi, *Cancers*, 2023, **15**, 4944. For selected examples: see: ; (*h*) L. Evangelista, G. Jori, D. Martini and G. Sotti, *Appl. Radiat. Isot.*, 2013, **74**, 91–101; (*i*) G. Chen, J. Yang, G. Lu, P. C. Liu, Q. Chen, Z. Xie and C. Wu, *Mol. Pharm.*, 2014, **11**, 3291–3299; (*j*) P. Hoppenz, S. Els-Heindl, M. Kellert, R. Kuhnert, S. Saretz, H.-G. Lerchen, J. Köbberling, B. Riedl, E. Hey-Hawkins and A. G. Beck-Sickinger, *J. Org. Chem.*, 2020, **85**, 1446–1457; (*k*) R. Li, J. Zhang, J. Guo, Y. Xu, K. Duan, J. Zheng, H. Wan, Z. Yuan and H. Chn, *Mol. Pharm.*, 2020, **17**, 202–211; (*l*) F. Zhao, K. Hu, C. Shao and G. Jin, *Polym. Test.*, 2021, **100**, 107269.

8 For selected recent applications in materials science, see: (*a*) B. P. Dash, R. Satapathy, E. R. Gaillard, K. M. Norton, J. A. Maguire, N. Chug and N. S. Hosmane, *Inorg. Chem.*, 2011, **50**, 5485–5493; (*b*) A. M. Spokoyny, C. W. Machan, D. J. Clingerman, M. S. Rosen, M. J. Wiester, R. D. Kennedy, C. L. Stern, A. A. Sarjeant and C. A. Mirkin, *Nat. Chem.*, 2011, **3**, 590–596; (*c*) K.-R. Wee, Y.-J. Cho, S. Jeong, S. Kwon, J.-D. Lee, I.-H. Suh and S. O. Kang, *J. Am. Chem. Soc.*, 2012, **134**, 17982–17990; (*d*) A. M. Spokoyny, C. D. Lewis, G. Teverovskiy and S. L. Buchwald, *Organometallics*, 2012, **31**, 8478–8481; (*e*) C. A. Lugo, C. E. Moore, A. L. Rheingold and V. Lavallo, *Inorg. Chem.*, 2015, **54**, 2094–2096; (*f*) H. Naito, Y. Morisaki and Y. Chujo, *Angew. Chem., Int. Ed.*, 2015, **54**, 5084–5087; (*g*) J. C. Axtell, O. Kirlikovali, P. I. Djurovich, D. Jung, V. T. Nguyen, B. Munekiyo, A. T. Royappa, A. L. Rheingold and A. M. Spokoyny, *J. Am. Chem. Soc.*, 2016, **138**, 15758–15765; (*h*) H. A. Mills, C. G. Jones, K. P. Anderson, A. D. Ready, P. I. Djurovich, S. I. Khan, J. N. Hohman, H. M. Nelson and A. M. Spokoyny, *Chem. Mater.*, 2022, **34**, 6933–6943; (*i*) M. Y. Tsang, S. Rodríguez-Hermida, K. C. Stylianou, F. Tan, D. Negi, F. Teixidor, C. Viñas, D. Choquesillo-Lazarte, C. Verdugo-Escamilla, M. Guerrero, J. Sort, J. Juanhuix, D. Maspoch, J. G. Planas, J. Sort, J. Juanhuix, D. Maspoch and J. G. Planas, *Cryst. Growth Des.*, 2017, **17**, 846–857; (*j*) E. Oleshkevich, F. Teixidor, A. Rosell and C. Viñas, *Inorg. Chem.*, 2018, **57**, 462–470; (*k*) K. L. Martin, J. N. Smith, E. R. Young and K. R. Carter, *Macromolecules*, 2019, **52**, 7951–7960; (*l*) L. Gan, A. Chidambaram, P. G. Fonquernie, M. E. Light, D. Choquesillo-Lazarte, H. Huang, E. Solano, J. Fraile, C. Viñas, F. Teixidor, J. A. R. Navarro, K. C. Stylianou and J. G. Planas, *J. Am. Chem. Soc.*, 2020, **142**, 8299–8311; (*m*) D. Tu, J. Li, F. Sun, H. Yan, J. Poater and M. Solà, *JACS Au*, 2021, **1**, 2047–2057; (*n*) J. Ochi, K. Tanaka and Y. Chujo, *Inorg. Chem.*, 2021, **60**, 8990–8997; (*o*) M. A. Waddington, X. Zheng, J. M. Stauber, E. Hakim Moully, H. R. Montgomery, L. M. A. Saleh, P. Král and A. M. Spokoyny, *J. Am. Chem. Soc.*, 2021, **143**, 8661–8668; (*p*) L. Gan, E. Andres-Garcia, G. Mínguez Espallargas and J. G. Planas, *ACS Appl. Mater. Interfaces*, 2023, **15**, 5309–5316; (*q*) X. Xu, Q. Cui, H. Chen and N. Huang, *J. Am. Chem. Soc.*, 2023, **145**, 24202–24209; (*r*) K. B. Idrees, K. O. Kirlikovali, C. Setter, H. Xie, H. Brand, B. Lal, F. Sha, C. S. Smoljan, X. Wang, T. Islamoglu, L. M. Macreadie and O. K. Farha, *J. Am. Chem. Soc.*, 2023, **145**, 23433–23441; (*s*) P.-F. Cui, X.-R. Liu and G.-X. Jin, *J. Am. Chem. Soc.*, 2023, **145**, 19440–19457; (*t*) L. Gan, M. T. Nord, J. M. Lessard, N. Q. Tufts, A. Chidambaram, M. E. Light, H. Huang, E. Solano, J. Fraile, F. Suárez-García, C. Viñas, F. Teixidor, K. C. Stylianou and J. G. Planas, *J. Am. Chem. Soc.*, 2023, **145**, 13730–13741; (*u*) K. Liu, J. Zhang, Q. Shi, L. Ding, T. Liu and Y. Fang, *J. Am. Chem. Soc.*, 2023, **145**, 7408–7415; (*v*) C. N. Kona, R. Oku, S. Nakamura, M. Miura, K. Hirano and Y. Nishii, *Chem*, 2023, **10**, 402–413; (*w*) F. Sun, S. Tan, H.-J. Cao, J. Xu, V. I. Bregadze, D. Tu, C. Lu and H. Yan, *Angew. Chem., Int. Ed.*, 2022, **61**, e202207125; (*x*) A. W. Tomich, J. Park, S.-B. Son, E. P. Kamphaus, X. Lyu, F. Dogan, V. Carta, J. Gim, T. Li, L. Cheng, E. Lee, V. Lavallo and C. S. Johnson, *Angew. Chem., Int. Ed.*, 2022, **61**, e202208158; (*y*) R. Jay, A. W. Tomich, J. Zhang, Y. Zhao, A. De Gorostiza, V. Lavallo and J. Guo, *ACS Appl. Mater. Interfaces*, 2019, **11**, 11414–11420; (*z*) M. Zhong, J. Zhou, H. Fang and P. Jena, *Phys. Chem. Chem. Phys.*, 2017, **19**, 17937–17943.

9 R. N. Grimes, *Carboranes*, Academic Press, New York, 3rd edn, 2016.

10 For reviews on the direct carborane B–H functionalizations, see: (*a*) Z. Qiu and Z. Xie, *Acc. Chem. Res.*, 2021, **54**, 4065–4079; (*b*) Y. K. Au and Z. Xie, *Bull. Chem. Soc. Jpn.*, 2021, **94**, 879–899; (*c*) J. Zhang and Z. Xie, *Sci. Sin. Chim.*, 2023, **53**, 312–319; (*d*) J. Zhang and Z. Xie, *Adv. Catal.*, 2022, 91–167; (*e*) Y. Quan and X. Xie, *Chem. Soc. Rev.*, 2019, **48**, 3660–3673; (*f*) X. Zhang and H. Yan, *Coord. Chem. Rev.*, 2019, **378**, 466–482; (*g*) S. Duttwyler, *Pure Appl. Chem.*, 2018, **90**, 733–744. For selected recent examples, see: ; (*h*) H. Ren, P. Zhang, J. Xu, W. Ma, D. Tu, C.-S. Lu and H. Yan, *J. Am. Chem. Soc.*, 2023, **145**, 7638–7647; (*i*) M. Chen, J. Xu, D. Zhao, F. Sun, S. Tian, D. Tu, C. Lu and H. Yan, *Angew. Chem., Int. Ed.*, 2022, **61**, e202205672; (*j*) Y.-N. Ma, H. Ren, Y. Wu, N. Li, F. Chen and X. Chen, *J. Am. Chem. Soc.*, 2023, **145**, 7331–7342; (*k*) S. Li and Z. Xie, *J. Am. Chem. Soc.*, 2022, **144**, 7960–7965; (*l*) H. A. Mills, J. L. Martin, A. L. Rheingold and A. M. Spokoyny, *J. Am. Chem. Soc.*, 2020, **142**, 4586–4591; (*m*) R. Cheng, B. Li, J. Wu, J. Zhang, Z. Qiu, W. Tang, S.-L. You, Y. Tang and Z. Xie, *J. Am. Chem. Soc.*, 2018, **140**, 4508–4511; (*n*) R. Cheng, J. Zhang, H. Zhang, Z. Qiu and Z. Xie, *Nat. Commun.*, 2021, **12**, 7146; (*o*) H. Lyu, J. Zhang, J. Yang, Y. Quan and Z. Xie, *J. Am. Chem. Soc.*, 2019, **141**, 4219–4224; (*p*) F. Lin, J.-L. Yu, Y. Shen, S.-Q. Zhang, B. Spingler, J. Liu, X. Hong and

S. Duttwyler, *J. Am. Chem. Soc.*, 2018, **140**, 13798–13807; (*q*) Y. Zhang, T. Wang, L. Wang, Y. Sun, F. Lin, J. Liu and S. Duttwyler, *Chem.–Eur. J.*, 2018, **24**, 15812–15817; (*r*) Y.-F. Liang, L. Yang, B. B. Jei, R. Kuniyil and L. Ackermann, *Chem. Sci.*, 2020, **11**, 10764–10769; (*s*) P.-F. Cui, X.-R. Liu, S.-T. Guo, Y.-J. Lin and G.-X. Jin, *J. Am. Chem. Soc.*, 2021, **143**, 5099–5105; (*t*) F. Lin, J.-L. Yu, Y. Shen, S.-Q. Zhang, B. Spingler, J. Liu, X. Hong and S. Duttwyler, *J. Am. Chem. Soc.*, 2018, **140**, 13798–13807; (*u*) Y. Baek, K. Cheong, G. H. Ko, G. U. Han, S. H. Han, D. Kim, K. Lee and P. H. Lee, *J. Am. Chem. Soc.*, 2020, **142**, 9890–9895.

11 For recent reviews on cross-couplings with halogenated carboranes and boron clusters, see: (*a*) R. M. Dziedzic and A. M. Spokoyny, *Chem. Commun.*, 2019, **55**, 430–442; (*b*) Y. Ge, J. Zhang, Z. Qiu and Z. Xie, *Dalton Trans.*, 2021, **50**, 1766–1773; (*c*) M. K. Al-Joumhawy, T. Marei, A. Shmalko, P. Cendoya, J. La Borde and D. Gabel, *Chem. Commun.*, 2021, **57**, 10007–10010; (*d*) K. P. Anderson, P. I. Djurovich, V. P. Rubio, A. Liang and A. M. Spokoyny, *Inorg. Chem.*, 2022, **61**, 15051–15057; (*e*) X. Mu, M. Hopp, R. M. Dziedzic, M. A. Waddington, A. L. Rheingold, E. M. Sletten, J. C. Axtell and A. M. Spokoyny, *Organometallics*, 2020, **39**, 4380–4386; (*f*) S. Li, Y. Liu and Z. Xie, *Chin. J. Chem.*, 2023, **42**, 129–134; (*g*) Y. Ge, J. Zhang, Z. Qiu and Z. Xie, *Angew. Chem., Int. Ed.*, 2020, **59**, 4851–4855.

12 (*a*) M. A. Fox and K. Wade, *J. Organomet. Chem.*, 1999, **573**, 279–291; (*b*) J. Yoo, J.-W. Hwang and Y. Do, *Inorg. Chem.*, 2001, **40**, 568–570; (*c*) R. M. Dziedzic, J. C. Axtell, A. L. Rheingold and A. M. Spokoyny, *Org. Process Res. Dev.*, 2019, **23**, 1638–1645.

13 (*a*) W. J. Marshall, R. J. Young and V. V. Grushin, *Organometallics*, 2001, **20**, 523–533; (*b*) K. Ishita, A. Khalil, R. Tiwari, J. Gallucci and W. Tjarks, *Eur. J. Inorg. Chem.*, 2018, **24**, 2821–2825; (*c*) Y. Sevryugina, R. L. Julius and M. F. Hawthorne, *Inorg. Chem.*, 2010, **49**, 10627–10634.

14 R. M. Dziedzic, L. M. A. Saleh, J. C. Axtell, J. L. Martin, S. L. Stevens, A. T. Royappa, A. L. Rheingold and A. M. Spokoyny, *J. Am. Chem. Soc.*, 2016, **138**, 9081–9084.

15 R. M. Dziedzic, J. L. Martin, J. C. Axtell, L. M. A. Saleh, T.-C. Ong, Y.-F. Yang, M. S. Messina, A. L. Rheingold, K. N. Houk and A. M. Spokoyny, *J. Am. Chem. Soc.*, 2017, **139**, 7729–7732.

16 (*a*) Y.-N. Ma, Y. Gao, Y. Ma, Y. Wang, H. Ren and X. Chen, *J. Am. Chem. Soc.*, 2022, **144**, 8371–8378; (*b*) J. Zhang and Z. Xie, *Angew. Chem., Int. Ed.*, 2022, **61**, e202202675; (*c*) Y. Ki Au, Q. Ma, J. Zhang and Z. Xie, *Chem.–Asian J.*, 2023, **18**, e202300611; (*d*) Y. K. Au, J. Zhang, Y. Quan and Z. Xie, *J. Am. Chem. Soc.*, 2021, **143**, 4148–4153; (*e*) A. Kataki-Anastasakou, J. C. Axtell, S. Hernandez, R. M. Dziedzic, G. J. Balaich, A. L. Rheingold, A. M. Spokoyny and E. M. Sletten, *J. Am. Chem. Soc.*, 2020, **142**, 20513–20518; (*f*) H. Lyu, Y. Quan and Z. Xie, *J. Am. Chem. Soc.*, 2016, **138**, 12727–12730; (*g*) G. U. Han, Y. Baek, K. Lee, S. Shin, H. Noh and P. H. Chan Lee, *Org. Lett.*, 2021, **23**, 416–420; (*h*) H. Lyu and Z. Xie, *Chem. Commun.*, 2022, **58**, 8392–8395.

17 For recent examples, see: (*a*) C. Maeng, G. H. Ko, H. Yang, S. H. Han, G. U. Han, H. Noh, K. Chan Lee, D. Kim and P. H. Lee, *Org. Lett.*, 2022, **24**, 3526–3531; (*b*) J. Zhang and Z. Xie, *Chem. Sci.*, 2021, **12**, 5616–5620; (*c*) C. X. Cui, J. Zhang, Z. Qiu and Z. Xie, *Dalton Trans.*, 2020, **49**, 1380–1383; (*d*) R. Cheng, Z. Qiu and Z. Xie, *Chin. J. Chem.*, 2020, **38**, 1575–1578; (*e*) R. Zhang, Y. Yuan, Z. Qiu and Z. Xie, *Chin. J. Chem.*, 2018, **36**, 273–279; (*f*) J. Zhang, Z. Qiu and Z. Xie, *Organometallics*, 2017, **36**, 3806–3811; (*g*) D. Zhao, J. Zhang and Z. Xie, *J. Am. Chem. Soc.*, 2015, **137**, 13938–13942; (*h*) S. Ren, Z. Qiu and Z. Xie, *Organometallics*, 2013, **32**, 4292–4300; (*i*) J. H. Wright, C. E. Kefalidis, F. S. Tham, L. Maron and V. Lavallo, *Inorg. Chem.*, 2013, **52**, 6223–6229; (*j*) M. Asay, C. E. Kefalidis, J. Estrada, D. S. Weinberger, J. Wright, C. E. Moore, A. L. Rheingold, L. Maron and V. Lavallo, *Angew. Chem., Int. Ed.*, 2013, **52**, 11560–11563; (*k*) S. Yruegas, J. C. Axtell, K. O. Kirlikovali, A. M. Spokoyny and C. D. Martin, *Chem. Commun.*, 2019, **55**, 2892–2895; (*l*) Y. Nie, J. Miao, H. Wadepohl, H. Pritzkow, T. Oeser and W. Siebert, *Z. Anorg. Allg. Chem.*, 2013, **639**, 1188–1193; (*m*) H. Zhang, J. Wang, W. Yang, L. Xiang, W. Sun, W. Ming, Y. Li, Z. Lin and Q. Ye, *J. Am. Chem. Soc.*, 2020, **142**, 17243–17249; (*n*) C. Zhang, J. Wang, W. Su, Z. Lin and Q. Ye, *J. Am. Chem. Soc.*, 2021, **143**, 8552–8558; (*o*) J. Krebs, A. Häfner, S. Fuchs, X. Guo, F. Rauch, A. Eichhorn, I. Krummenacher, A. Friedrich, L. Ji, M. Finze, Z. Lin, H. Braunschweig and T. B. Marder, *Chem. Sci.*, 2022, **13**, 14165–14178; (*p*) J. Wang, L. Xiang, X. Liu, A. Matler, Z. Lin and Q. Ye, *Chem. Sci.*, 2024, **15**, 4839–4845; (*q*) Y. Li, M. Tamizmani, M. O. Akram and C. D. Martin, *Chem. Sci.*, 2024, 10, DOI: **10.1039/D4SC00990H**.

18 (*a*) J. Poater, C. Vinas, M. Sola and F. Teixidor, *Nat. Commun.*, 2022, **13**, 3844; (*b*) T. L. Chan and Z. Xie, *Chem. Sci.*, 2018, **9**, 2284–2289.

 